

Identification of a Discrete-Time Nonlinear Hammerstein-Wiener Model for a Selective Catalytic Reduction System

Darine Zambrano, Soma Tayamon, Bengt Carlsson and Torbjörn Wigren

Abstract—This paper deals with the identification of the nitrogen oxide emissions (NO_x) from vehicles using the selective catalyst as an aftertreatment system for its reduction. The process is nonlinear, since the chemical reactions involved are highly depending on the operating point. The operating point is defined by the driving profile of the vehicle, which includes for example, cold and hot engine starts, highway, and urban driving. The experimental data used in this paper are based on a standard transient test developed for Euro VI testing. Real measurements of NO_x inlet concentration, injected urea, inlet temperature and exhaust flow are used as inputs to a detailed simulator. NO_x output concentration from the simulator is used as output, so there is no interference from the ammonia concentration in the NO_x output concentration due to cross-sensitivity. Experimental data are properly divided into identification and validation data sets. A Hammerstein-Wiener model is identified and it represents the dynamics very well. The best fits achieved with this model are 78.64% and 68.05% for the identification and validation data, respectively. Nonlinear static functions are selected from the knowledge and analysis of a selective catalytic reduction first principles based model. Identified linear models are able to represent the NO_x emission with a fit of 68.93% and 38.92% for the identification and validation data, respectively.

I. INTRODUCTION

NO_x emissions in exhaust gases adversely affect the environment, since NO_x contributes to the formation of acid rain and ground level ozone, among others. To prevent damages to the environment and human health, emission standards for a number of atmospheric pollutants, as NO_x , have been established decades ago and they are stringently updated. One of the technologies used for NO_x control is the selective catalytic reduction (SCR). This technology has been developed from the 50's, using several components for the catalyst (e.g. vanadium, titanium) and several reducing agents (e.g. ammonia), and it has been employed successfully in power plants, furnaces, gas turbines and automotive applications. Among the current technologies, SCR is the more convenient one for heavy-duty applications, but optimal operation is required to meet new emission targets [1]. [2] introduced Euro VI emission standards, and they become effective from 2013 and 2014. The proposed limit value for NO_x emissions is 0.4 g/kWh for heavy-duty engines.

Numerous authors have contributed in the development of detailed and complex models for SCR systems, see e.g. the lumped parameter model developed by [3]. Recently, [4] presented a transient kinetic model for SCR of NO_x with

ammonia over an Fe-zeolite catalyst for a wide range of temperatures (i.e. 150°C to 650°C). In [5], a simplified dynamic model of a three-way catalytic converter is developed and validated against dynamic A/F (air/fuel) and emissions data. In [6], a detailed model for diesel engines is developed and validated, including the SCR catalyst model, model based optimization is applied to minimize brake specific fuel consumption including urea cost while maintaining NO_x and NH_3 emissions at Euro VI levels. A model describing exhaust gas temperature, molar flows of NO_x and NH_3 downstream of the treatment system for variations in the engine power and constant engine speed was developed in [7]. [8] illustrates a transient model of SCR monolith reactors for automotive applications, which is validated against data at different scales, including engine test bench experiments. Also, the dynamic effects at low temperatures are analysed. There are numerous kinetic models in the literature, which often require several and specific tests for determining the parameters of the model. From the point of view of control, it is however attractive to obtain simpler models that can be used more easily in controller design. [9], for example, shows the NO_x emission prediction from the diesel engine operating variables by using a neural network, the split and fit algorithm and a polynomial NARX algorithm, but the SCR system is not treated.

Optimal performance of SCR is a challenging problem, with many research efforts being made. An interesting analysis of the closed loop SCR control from a practical control point of view is illustrated in [1], where also three control strategies are evaluated using a simulator. [10] presents a combination of feedforward and feedback control structures for a SCR process using software sensors for measurements of the nitric oxide concentration at the input of the catalytic converter and the flue gas flow rate. [11] presents a model-based feedforward controller. The issue of the cross-sensitivity in NO_x sensors is analysed in [12]. Ammonia coverage ratio is estimated by the use of nonlinear observers in [13]. These works highlight the need of using advanced control strategies to meet the stringent requirements.

The objective of this paper is to model the dynamics of the NO_x emissions in the exhaust gas aftertreatment system for the changing operating conditions exhibited in automotive applications. A main idea is to use a simple model structure, thereby facilitating controller design. Promising results using nonlinear Hammerstein-Wiener models [14] are reported in this paper. Another noteworthy aspect is that the model uses an exponential function of the temperature to scale the effect of the input temperature. Hammerstein-Wiener models have

The authors are with the Division of Systems and Control, Department of Information Technology, Uppsala University, SE-75105 Uppsala, Sweden (e-mail: {darine.zambrano, soma.tayamon, bengt.carlsson, torbjorn.wigren}@it.uu.se)

also been used successfully in other chemical processes as for example [15], [16]. The main contribution of this work is hence the development of simpler, yet accurate, models for NO_x in the aftertreatment flue gas having less estimated parameters than those available in the literature and that can be estimated from regular operating data. The fact that few parameters need to be estimated simplifies controller design and is particularly important in case adaptive control is attempted.

The paper is structured as follow: Section II describes the analysed process, specifically Subsection II-A illustrates the SCR system, and Subsection II-B details the experimental data set used for identification. Identified models are described in Section III. A comparison between the identification results is made in Section IV. Finally the conclusions are presented in Section V.

II. SELECTIVE CATALYTIC REDUCTION SYSTEM

A. Description

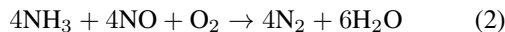
For automotive applications, the selective catalytic reduction exhaust gas aftertreatment system commonly consists of a honeycomb monolith, where several chemical reactions take place, combined with a dosification system of a reduction agent. Fig. 1 shows the main components of the system: the urea injection system, the catalyst and the sensors for exhaust flow, temperature and concentrations.

The SCR system consists of two main stages. Firstly, a reduction agent, in this case urea, is injected upstream through a nozzle and mixed with the exhaust flow at the input of the catalyst. Urea is contained in a harmless aqueous solution commercially named AdBlue, which consist of 32.5% urea. Urea is converted to ammonia as is shown in the following reaction (1):

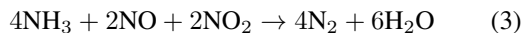


Secondly, the ammonia is partially adsorbed on the surface of the catalyst, where finally the dominant reactions occur in the catalyst, i.e. the ammonia reacts with the NO_x emitted by the engine (NO_x is composed primarily of NO with lesser amounts of NO_2) in order to get nitrogen gas (N_2) and water (H_2O) as final products:

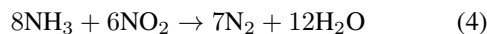
- Standard SCR reaction



- Fast SCR reaction



- NO_2 SCR reaction



The efficiency of the SCR system is usually evaluated by the amount of NO_x reduced within the catalyst, see (5) (C is concentration), and by the ammonia slip, which represents the unreacted ammonia. Only the first measure is used in this paper.

$$\% \text{NO}_{x,r} = \frac{C_{\text{NO}_{x,\text{in}}} - C_{\text{NO}_{x,\text{out}}}}{C_{\text{NO}_{x,\text{in}}}} \times 100 \quad (5)$$

The optimal operation of a SCR system requires taking into account the complex relationships governing the products formation. There are many factors affecting these formations. The amount of formed NH_3 depends on temperature and space velocity [17]. The homogeneous injected urea distribution improves the NO_x conversion. For low temperatures NO_x conversion is decreased. Some undesirable products can be formed depending on the temperature value (see [1]), NH_3 oxidation is produced for high temperatures ($>450^\circ\text{C}$), and ammonium nitrate (NH_4NO_3) and nitrous oxide (N_2O) are formed at respectively temperatures below 200°C and above 450°C . In automotive applications the temperature can vary significantly, from the cold start of the engine until hot operating conditions.

B. Experimental test

The World Harmonized Transient Cycle (WHTC) [18] will be used for Euro VI testing. For this reason, it was used for the identification test in this paper. The WHTC is a transient test with a length of 1800 s which specifies engine speed and load values. It starts with a highly transient part (urban driving) and ends with higher load and less transience (highway driving). Fig. 2 shows the NO_x at the output of the catalyst obtained from the simulator, which is the model output (y_r) [fraction], and the four signals used as inputs, i.e. NO_x concentration at inlet ($u_{r,1}$) [fraction], the injected urea ($u_{r,2}$) [g/min], the temperature ($u_{r,3}$) [K] and the exhaust flow ($u_{r,4}$) [mol/s]. From Fig. 2, it can be noticed that the exhaust flow exhibits steady values and high frequency changes. The amount of injected urea is related to the NO_x input concentration and to the exhaust flow. It can be noticed that its value is zero during some time intervals, specifically for low exhaust flow or low NO_x input concentration. Also, the temperature changes smoothly for a broad range of values, i.e. 470 K to 670 K approximately (200°C to 400°C approximately). A detailed explanation of the simulator used can be found in [6]. The advantage of using this simulator is that several input signals can be tested, and the issue of the cross-sensitivity in the NO_x output sensor due to the presence of ammonia is avoided. Recent publications about available NO_x sensors, e.g. [12], have shown that they are affected significantly by the amount of ammonia at the output of the tailpipe. This issue can create instability problems in closed-loop control using such sensors for feedback. Fig. 3 shows the percentage of NO_x reduction for the data set used. It can be observed that the NO_x conversion is highly affected by the changes in the engine variables and the injected urea. The plot illustrates the difficulty to be able to keep high NO_x conversion ($>80\%$) coping with these varying operating conditions.

III. IDENTIFICATION

A. Data preprocessing

Table I shows the values used for preprocessing of the inputs and the output. The original data have been processed to have zero mean and standard deviation (SD) one. In this paper, the first 900 samples have been used for identification

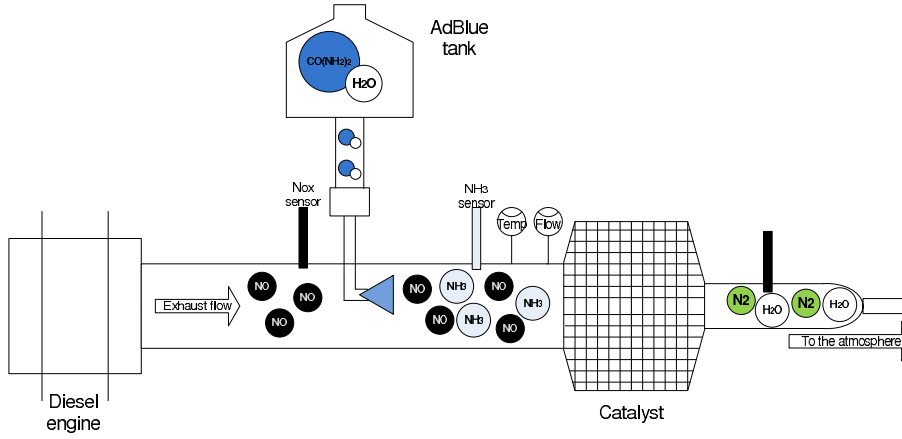


Fig. 1. SCR system.

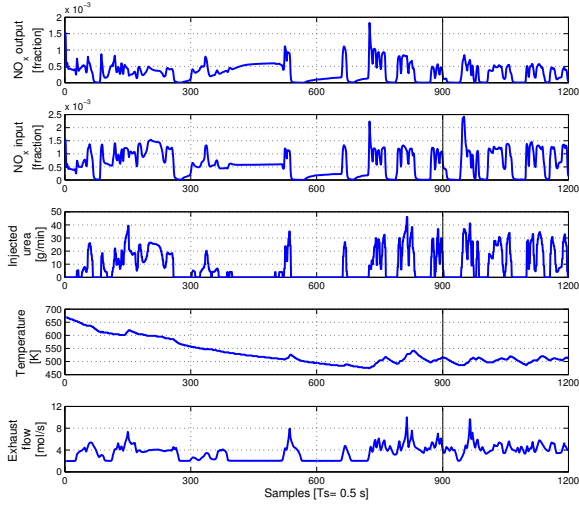


Fig. 2. Experimental data.

TABLE I
VALUES USED FOR PREPROCESSING

Variable	y_r	$u_{r,1}$	$u_{r,2}$	$u_{r,3}$	$u_{r,4}$
Mean	0.325×10^{-3}	0.619×10^{-3}	8.418	533.97	3.596
SD	0.2667×10^{-3}	0.482×10^{-3}	11.212	48.130	1.338

and the last 300 samples for validation (see the boundary line in Fig. 2 at sample 900). The sampling time is 500 ms. The preprocessed variables are denoted by y , u_1 , u_2 , u_3 and u_4 respectively.

B. Linear models

Two linear models were estimated (M-I and M-II), in order to evaluate what is the best behaviour achieved with linear models. u_1 , u_2 , u_3 and u_4 are considered as model inputs, and y as model output. State space (M-I) and output-error (M-II) models were obtained using Matlab commands, p_{em} (prediction-error method (PEM)) and o_e (output-error

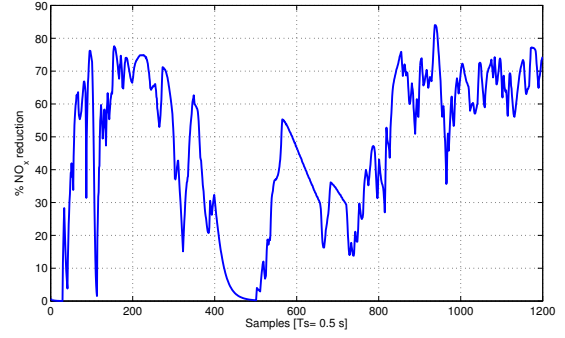


Fig. 3. Percentage of NO_x reduction for the experimental data set.

(OE)), respectively, from the System Identification Toolbox. The first one, p_{em} , estimates the parameters of a state space model based on iterative minimization of a criterion. The second one, o_e , estimates the parameters of an output-error (OE) model using the prediction error method, for more details see [14], [19].

1) *State space model (M-I)*: The state space model is obtained by the minimization of the quadratic error between the measured output and the estimated output. The discrete time state-space model is as follows:

$$\begin{aligned} x(t+1) &= \mathbf{A}x(t) + \mathbf{B}u(t) \\ y(t) &= \mathbf{C}x(t) + \mathbf{D}u(t) \end{aligned} \quad (6)$$

where \mathbf{A} , \mathbf{B} , \mathbf{C} , \mathbf{D} are the system matrices with proper dimensions, $x(t)$ is the state vector and t is discrete time. The number of states is 2. There was no significant improvement when the number of states was increased.

2) *Output-error model (M-II)*: The parameter coefficients were obtained using the prediction error method in which the minimized criterion is the square of the error, normalized by the length of the data set. The structure of a general multiple-input single-output (MISO) output-error

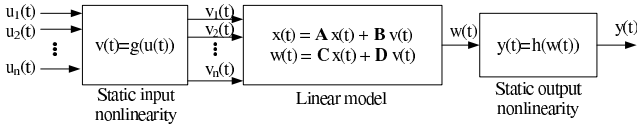


Fig. 4. Hammerstein-Wiener model block diagram.

model takes the following form,

$$y(t) = \sum_{i=1}^n \frac{B_i(z^{-1})}{F_i(z^{-1})} u_i(t) + e(t) \quad (7)$$

where $y(t)$, $u_i(t)$ and $e(t)$ are the system output, inputs and noise respectively, and n is the number of inputs for a MISO system. $B_i(z^{-1})$ and $F_i(z^{-1})$ are polynomials defined in the backward shift operator z^{-1} . The order chosen for B_i and F_i was 1 and 2 respectively, with delays set to zero and n selected as 4.

C. Non-linear models: Hammerstein-Wiener model (M-III, M-IV, M-V)

As linear models are not able to accurately describe the NO_x behaviour for these transient conditions, static non-linear functions were included by the use of Wiener and Hammerstein-Wiener models. In general, a Hammerstein-Wiener model is comprised of three blocks: a static input nonlinearity (from Hammerstein model), a linear dynamic system, and a static output nonlinearity (from Wiener model). For more information see ([20], [21], [22], [14]). Fig. 4 shows the connection between these blocks. Static nonlinearities ($g(\cdot)$ and $h(\cdot)$) can be identified using black-box techniques, or be fixed from the knowledge of the process. The advantage of using these independent blocks is that they can be fixed in an individual way, even the static nonlinearities in multivariable systems. The linear model in Fig. 4 is represented by a state space model, but any linear model can be used in this block. A Wiener model (M-III) and two Hammerstein-Wiener models (M-IV and M-V) were identified. The identification was performed with the Matlab command `nlhw` of the System Identification toolbox.

1) *Static nonlinear output function:* The static output nonlinearity is chosen as a saturation function (8), since negative values for NO_x concentration are not physical. They are observed in the linear model response. The lower limit (w_{\min}) is set as the ratio between the negative mean value and the standard deviation of y_r , which corresponds to NO_x concentration equal to zero.

$$y(t) = \begin{cases} w(t) & \text{for } w(t) > w_{\min} \\ w_{\min} & \text{for } w(t) \leq w_{\min} \end{cases} \quad (8)$$

This saturation function was used for the M-III, M-IV and M-V models.

2) *Static nonlinear input functions:* (a) For the model M-III, static nonlinear input functions are not set as it is a Wiener model. (b) For the M-IV identified model, the static input nonlinearity is fixed only for the temperature (the other inputs enter linearly), and it is expressed in the same way

that temperature is involved in the chemical reaction rates in the first principle based model (see (10)). It is well-known that there are several chemical reaction rates, so the value of a has been fixed in order to have a value of the same order as in the first principle based model presented in [11] for the standard SCR reaction (2). The value of a was set as 10^4 K. The idea is to use the kinetic equations to fix the shape of the nonlinearities, but the idea is not to have a physical explanation for each one of these. The static input nonlinearity $v_{3,IV}(t)$ for the model M-IV is the exponential of the negative scaled inverse of the temperature expressed in Kelvin (see (10)). Therefore, for the model M-IV, the inputs of the static nonlinearity function $g(\cdot)$ are the real inputs $u_{r,i}(t)$, and $v_{i,IV}(t)$ are the preprocessed variables having zero mean and SD one. Mean and SD values are the same as in Table I, except for $v_{3,IV}(t)$ that has 2.614×10^{-8} as mean value and 5.372×10^{-8} as SD. Hence

$$v_{i,IV}(t) = u_i(t) \quad \text{for } i = 1, 2, 4 \quad (9)$$

$$v_{3,IV}(t) = e^{(-a/u_3(t))} \quad (10)$$

(c) For the model M-V, the input nonlinearity given by (10) was retained for the set-up of the input nonlinear functions, as it showed to be a beneficial choice. Piecewise linear (PWL) functions as static nonlinear function in block-oriented models have shown to be a versatile and effective alternative ([23], [24]). This is employed in M-V here. The previous inputs $v_{i,IV}(t)$ from (9) and (10) are used for the PWL estimation. The input set of signals for the linear block of the model M-V is given by the PWL function $v_{i,V}(t)$ defined as (11):

$$v_{i,V}(t) = c_j v_{i,IV}(t) + d_j \quad \forall \quad v_{i,IV} \in R_j, \quad (11) \\ \text{for } j = 1, 2, \dots, N_i.$$

where R_1, \dots, R_{N_i} are partitions of \mathfrak{R} . For the model M-V, the number of partitions are $\{N_1, N_2, N_3, N_4\} = \{9, 5, 9, 5\}$. The fact that the piecewise model consists of 56 parameters requires special consideration of validation, see Section IV.

3) *Linear model:* In this paper, the linear dynamic system for the models M-III, M-IV and M-V is represented by (7), with $w(t)$ as the system output and $v_i(t)$ as the systems inputs ($i = 1, 2, 3, 4$). The parameters of the linear model were fitted for each model.

IV. RESULTS AND ANALYSIS

Figs. 5 and 6 show the output for the different models for the identification data set as well as validation data set in the units of the measured variable. In Fig. 5, it can be observed that the major deficiency of the linear models (M-I and M-II) is in the estimation of low values of NO_x , but their behaviour for high frequency changes at intermediate values, as between 100 and 250 samples, are reasonably good. From Fig. 6 can be noticed that some peaks using the validation data set have higher values for the identified linear models than for the output from the simulator. As the performance criteria used (see Table II) showed a slightly better overall performance for the OE model (M-II), this

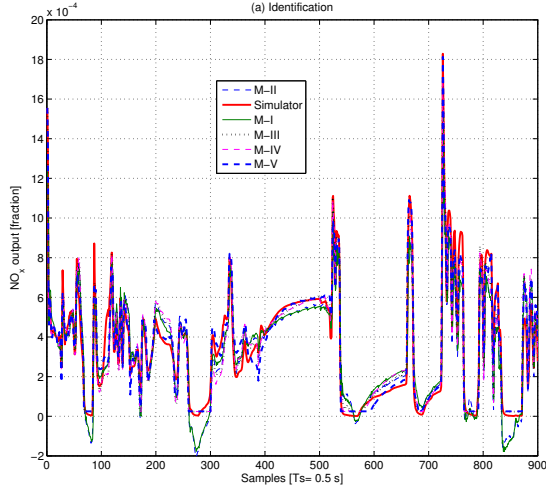


Fig. 5. NO_x output for the identified models using the identification data set.

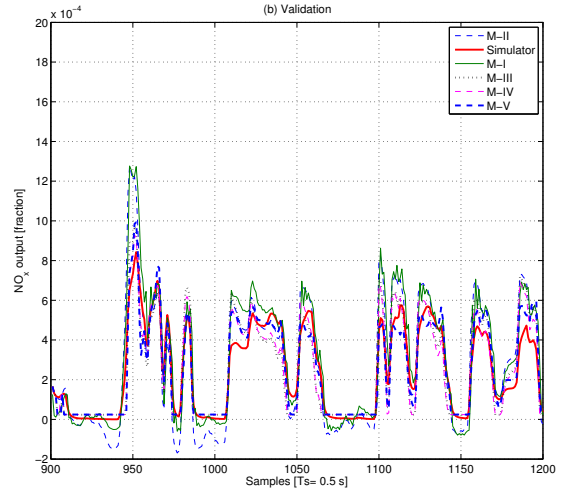


Fig. 6. NO_x output for the identified models using the validation data set.

structure was used as linear model for the Wiener and Hammerstein-Wiener models. As the main source of error is observed for low values of NO_x , the next step was to include a saturation function as the static output nonlinearity of a Wiener model as in [25]. Figs. 5 and 6 show for the Wiener model (M-III) that negative values in the NO_x output were eliminated and the peaks in the validation data set are closer to the real output than with the linear models. In order to improve the NO_x estimation, a static input nonlinearity was considered for the temperature in the first Hammerstein-Wiener model (M-IV). The outcome of this static nonlinear function is stressing the effect of the temperature for high values and minimizing its effect for low temperatures. It can be noticed that the NO_x estimation is better than using the other identified models, and, that an undesired ripple on the previous output signal is eliminated. The NO_x estimation was hence improved with this input nonlinearity. The best results were obtained for the second Hammerstein-Wiener model (M-V) by incorporating PWL functions to the static input functions. PWL functions are shown in Fig. 7.

To make a quantitative comparison, FIT and MSE values have been considered as performance criteria and they are defined as (12) and (13):

$$FIT = \left(1 - \frac{\|y_r - y\|_2}{\|y_r - \bar{y}_r\|_2}\right) \times 100 \quad (12)$$

$$MSE = \frac{1}{N} \sum_{t=1}^N (y(t) - y_r(t))^2 \quad (13)$$

where y is the identified output, y_r is the output from the simulator, N is the number of samples, and $\|\cdot\|_2$ denotes the spectral norm.

Table II summarizes the values of FIT and MSE obtained for the each model. It can be observed that the best FIT for the validation data set is 66.80% for the Hammerstein-Wiener model (M-V). Notice that the difference between the

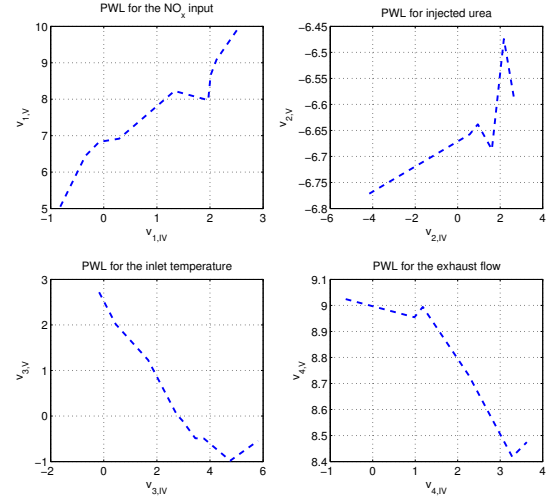


Fig. 7. PWL functions as static nonlinear input functions for model M-V.

FIT for the linear output-error model and the Hammerstein-Wiener model is 22.11%, which results in a significant improvement since both linear models have the same number of parameters, and the added static nonlinearities were relatively simple and intuitive, i.e. the saturation and the exponential functions. Besides, incorporation of the PWL functions allows to get an extra improvement of 6.16% and 7.02% over the results obtained with the model M-IV for the identification and validation data set respectively. It evidences the PWL ability to deal with nonlinear systems with changing operating points. In the same way the best MSE values are achieved for the Hammerstein-Wiener models. From the results it is concluded that M-V is probably not subject to overfit, despite the quite high number of parameters used.

TABLE II
RESULTS

Model	Identification		Validation	
	FIT	MSE	FIT	MSE
M-I	61.76%	0.156	40.33%	0.245
M-II	68.93%	0.103	38.92%	0.256
M-III	75.36%	0.065	55.67%	0.135
M-IV	72.48%	0.081	61.03%	0.104
M-V	78.64%	0.049	68.05%	0.070

V. CONCLUSION

The identified Hammerstein-Wiener models represent the NO_x behaviour for transient operating conditions quite well. Of all the candidate models studied, these nonlinear models provide a superior reproduction of the experimental data over the whole analysed period. Other appealing features of these Hammerstein-Wiener models lie in the simplicity of the nonlinearities considered and the possibility to include new nonlinearities, as well as in its easy implementation. These favorable results indicate that black-box simple models can estimate the NO_x emission.

The development of the proposed models can contribute to the development and implementation of nonlinear control strategies, which are needed to deal with the stringent specifications and dynamic operating conditions of automotive applications. It can be used in combination with robust controllers into a closed control loop structure, in order to deal with inaccuracies in NO_x measurements, as well as with unmodeled dynamics and time delay, and to improve accuracy in the urea dosage.

Future works include the analysis of more experimental data, including higher values for temperature. It could also be useful to improve the model structure and include delay estimation. Another future extension for this work is to include the ammonia slip as a new output of the model.

ACKNOWLEDGEMENTS

The authors would like to thank Scania AB for the data that is provided by them for identification and to the Swedish Energy Agency (project 32299-1) for partially supporting this work.

REFERENCES

- [1] F. Willems, R. Cloudt, E. van den Eijnden, M. van Genderen, R. Verbeek, B. de Jager, W. Boomsma, and I. van den Heuvel, "Is closed-loop SCR control required to meet future emission targets?" *SAE*, vol. 2007-01-1574, 2006.
- [2] The European Parliament and the Council, "Regulation (EC) No 595/2009 of the European parliament and of the Council," *Official Journal of the European Union*, pp. L 188/1 – L 188/13, June 2009.
- [3] E. Troconi, P. Forzatti, J. G. Martin, and S. Malloggi, "Selective catalytic removal of NO_x : A mathematical model for design of catalyst and reactor," *Chemical Engineering Science*, vol. 47, no. 9-11, pp. 2401–2406, 1992.
- [4] H. Sjövall, R. J. Blint, A. Gopinath, and L. Olsson, "A kinetic model for the selective catalytic reduction of NO_x with NH_3 over a Fe-zeolite catalyst," *Ind. Eng. Chem. Res.*, vol. 49, pp. 39–52, 2010.
- [5] E. P. Brandt, Y. Wang, and J. W. Grizzle, "Dynamic modeling of a three-way catalyst for SI engine exhaust emission control," *IEEE Transactions on Control Systems Technology*, vol. 8, no. 5, pp. 767–776, 2000.

- [6] C. Ericson, "Model based optimization of a complete diesel engine/SCR system," Ph.D. dissertation, Lund University, 2009.
- [7] C. M. Schär, C. H. Onder, and H. P. Geering, "Mean-value of the SCR system of a mobile application," in *15th IFAC World Congress*, Barcelona, Spain, July 2002.
- [8] E. Troconi, I. Nova, C. Ciardelli, D. Chatterjee, B. Bandl-Konrad, and T. Burkhardt, "Modelling of an SCR catalytic converter for diesel exhaust after treatment: Dynamics effects at low temperature," *Catalysis Today*, vol. 105, pp. 529–536, 2005.
- [9] H. C. Krijnsen, R. Bakker, W. E. J. van Kooten, H. P. A. Calis, R. P. Verbeek, and C. M. van den Bleek, "Evaluation of fit algorithms for NO_x emission prediction for efficient De NO_x control of transient diesel engine exhaust gas," *Ind. Eng. Chem. Res.*, vol. 39, pp. 2992–2997, 2000.
- [10] G. Dolanc, S. Strmcnik, and J. Petrovic, " NO_x selective catalytic reduction control based on simple models," *Journal of Process Control*, vol. 11, pp. 35–41, 2001.
- [11] C. M. Schär, C. H. Onder, and H. P. Geering, "Control of an SCR catalytic converter system for a mobile heavy-duty application," *IEEE Transactions on Control Systems Technology*, vol. 14, no. 4, pp. 641–653, 2006.
- [12] M. F. Hsieh and J. Wang, "An extended Kalman filter for NO_x sensor ammonia cross-sensitivity elimination in selective catalytic reduction applications," in *American Control Conference*, Baltimore, USA, June 30-July 02 2010.
- [13] —, "Nonlinear observer designs for diesel engine selective catalytic reduction (SCR) ammonia coverage ratio estimation," in *48th IEEE Conference on Decision and Control and 28th Chinese Control Conference*, Shanghai, P.R. China, December 2009.
- [14] L. Ljung, *System Identification - Theory for the User*, 2nd ed. Prentice-Hall, 1999.
- [15] H. H. J. Bloemen, C. T. Chou, T. J. J. van den Boom, V. Verdult, M. Verhaegen, and T. C. Backx, "Wiener model identification and predictive control for dual composition control of a distillation column," *Journal of Process Control*, vol. 11, no. 6, pp. 601 – 620, 2001.
- [16] G. Dolanc and S. Strmcnik, "Identification of nonlinear systems using a piecewise-linear Hammerstein model," *Systems and Control Letters*, vol. 54, no. 2, pp. 145 – 158, 2005.
- [17] J. N. Chi and H. F. DaCosta, "Modeling and control of a urea-SCR aftertreatment system," *SAE Transactions*, vol. 114, no. 4, pp. 449–464, 2005.
- [18] H. Steven, "Development of a worldwide harmonised heavy-duty engine emissions test cycle," United Nations, Tech. Rep., 2001.
- [19] L. Ljung, *System Identification Toolbox - for use with MATLAB, User's Guide*, 5th ed. The Mathworks, Inc. Sherborn, Mass, 2000.
- [20] S. A. Billings, "Identification of nonlinear systems: A survey," *Control Theory and Applications, IEE Proceedings D*, vol. 127, no. 6, pp. 272–285, 1980.
- [21] E.-W. Bai and M. Fu, "A blind approach to Hammerstein model identification," *IEEE Transactions on Signal Processing*, vol. 50, no. 7, pp. 1610–1619, 2002.
- [22] A. Hagenblad and L. Ljung, "Maximum likelihood estimation of Wiener models," in *Proceeding 39th IEEE Conference on Decision and Control*, 2000, pp. 2417–2418.
- [23] J. Vörös, *Block-oriented Nonlinear System Identification*, ser. Lecture Notes in Control and Computer Sciences. Springer-Verlag Berlin Heidelberg, 2010, vol. 404, ch. Compound Operator Decomposition and Its Application to Hammerstein and Wiener Systems, pp. 35–51.
- [24] R. K. Pearson and M. Pottmann, "Gray-box identification of block-oriented nonlinear models," *Journal of Process Control*, vol. 10, no. 4, pp. 301 – 315, 2000.
- [25] T. Wigren, "Convergence analysis of recursive identification algorithms based on the nonlinear Wiener model," *IEEE Transactions on Automatic Control*, vol. 39, no. 11, pp. 2191–2206, nov. 1994.